N.A. Smirnova [1], A.V. Korotun [1, 2], I.M. Titov [3]

AN INFLUENCE OF THE ADSORBED MOLECULES LAYER ON THE LOCALIZED SURFACE PLASMONS IN THE SPHERICAL METALLIC NANOPARTICLES

[1] National University Zaporizhzhia Polytechnic
64 Zhukovskogo Str., Zaporizhzhia, 69063, Ukraine, E-mail: andko@zp.edu.ua
[2] G.V. Kurdyumov Institute for Metal Physics of National Academy of Sciences of Ukraine
36 Academician Vernadsky Blvd., Kyiv, 03142, Ukraine
[3] UAD Systems
84 Oleksandrivska Str., Zaporizhzhia, 69002, Ukraine

An influence of the adsorbed molecules layer on the optical characteristics of the spherical metallic nanoparticles has been studied in the work. In order to do this one considers the additional term which takes into account the scattering of electrons at the interface between metal and adsorbate. The analytical expressions for the frequency dependences for the parameter of coherence loss due to the scattering at the interface "metal – adsorbed layer" have been obtained. It has been found that the presence of the adsorbed molecules results in the electron scattering anisotropy, and, hence, in the anisotropy of the optic response of such systems. The result of the indicated anisotropy is the appearance of the additional maximum in the infrared part of the spectrum in the frequency dependences for the optical characteristics. An evolution of the frequency dependences for the components of the polarizability tensor and the absorption cross-section and scattering cross-section for the two-layer spherical nanoparticles of the type "metal – adsorbate" under the variation of their geometrical parameters has been analyzed. It has been shown that the weak maximum of the real, imaginary parts and the module of the transverse component of the polarizability tensor and the absorption and scattering cross-sections in the infrared part of the spectrum appears due to inducing of the local density of the states by adsorbate. The reason of the shift of the maxima of the absorption cross-section and scattering cross-section for the nanoparticles of the constant sizes with the cores of different metals has been found. It has been demonstrated the existence of the small-scale oscillations at the frequency dependences for the components of the polarizability tensor and at the absorption and scattering cross-sections, caused by an oscillating contribution of the surface electron scattering. The dependence of the location and the value of the maximum of the absorption cross-section for the particle "metal – adsorbate" with the constant geometrical parameters and content on the dielectric permittivity of the medium, in which the nanoparticle is situated, has been proved.

Keywords: *composite nanoparticle, adsorbate, polarizability, absorption cross-section, scattering cross-section, surface plasmonic resonance, local density of the states*

INTRODUCTION

Nanoplasmonics has recently become an important area of the research in optics and material science with the different applications (chemical and biological sensors [1], surface-enhanced Raman spectroscopy [2, 3]), nanooptic devices [4–6] *etc*.), in which the unique optical characteristics of the plasmonic materials are used.

Metallic nanoparticles absorb and concentrate light energy in a small volume like a nanoscopic antenna [7]. The plasmonic oscillations are excited in the particle after the primary absorption of light. The energy of these oscillations is mainly re-emitted or converted into heat due to electron-electron and electron-photon scattering. In this case, the properties of the surface plasmons in nanoparticles depend on the properties of the adsorbed molecules of dielectrics, which surround them [8–10]. Thus, in some cases the energy of the plasmonic oscillations is converted into the transfer of electron towards the adsorbed material, which contributes to the generation of the electric currents [9, 10], gas dissociation [11], water splitting reactions [12], generation of higher optical harmonics [13], selective acceleration of the organic reactions [14], *etc*. It is believed that the transfer of electrons, induced by plasmons, takes place when plasmon decays into electron-hole pairs [15]. This process has low efficiency

because hot electrons quickly relax back to Fermi level, due to electron-electron scattering, before they can move to molecules on the surface of the nanoparticle. However, it has been shown in the recent work [16] that the excitation of plasmon can result in the direct transfer of electron into the loosened orbitals of adsorbate molecules and in the generation of the interfacial electron-hole pairs. This process makes the interfacial transfer of electrons, induced by plasmons, far more effective. Such direct way of electron transfer competes with the absorption and scattering. Hence, it is very important to quantify the relative contribution of these relaxation mechanisms in order to estimate and optimize the plasmonic properties of metallic nanoparticle for the practical use.

As is known, plasmons decay in 5–20 fs. Such rapid relaxation makes it difficult to investigate it directly in experiments with high temporal resolution [17]. An alternative to such measurements is to determine the width of the spectral line of the surface plasmonic resonance (SPR) of the individual nanoparticle [18], because the width of SPR line is directly proportional to the plasmon decay rate.

Four basic mechanisms of dissipation contribute into the width of SPR line [19]. They are bulk damping γ_{bulk}, radiation damping γ_{rad}, scattering on the surface γ_{surf} and the damping caused by the chemical interaction on the interface γ_{CID}.

The above mentioned mechanisms make the width of the plasmonic line the function of the shape of nanoparticle [20], optical properties of the material [21] and the environment [22]. Any method of the nanoparticle production, especially the wet chemical synthesis, leads to the significant size and shape distribution of the particles [23], which is the reason of the widening of SPR line, obtained under the studies of the nanoparticle ensembles. Therefore, only the width of SPR line, obtained in spectroscopy of the individual particles, is quantitatively related to the attenuation processes of the collective oscillations [24].

The attenuation at the chemical interface is the understudied relaxation mechanism. In [21] on the basis of the comparison of the plasmonic line width, measured for the ensemble of silver nanoparticles in the gas phase, and the particles, embedded into the matrix SiO_2 [21, 25, 26], it

was suggested that this mechanism is related to the capability of plasmon to decay due to the interaction with the interfacial electronic states. Recently in [16], the interfacial mechanism of the charge transfer, which is similar to the attenuation at the chemical interface, has been given in order to explain the high efficiency of the photoinitiated transfer of electrons from golden sphere to the attached nanorod CdSe.

Moreover, it is not clear whether the attenuation at the chemical interface and the scattering of electrons on the surface are two different phenomena or not, because both of them are related to the interface between metallic nanoparticle and its molecular surrounding. The studies of the ensembles of the nanoparticles, performed in [22], give the primary evidence that the attenuation at the chemical level also depends on the size. The classical model, which describes the scattering at the interface as an inelastic scattering on the surface of the nanoparticle, has been proposed later in [27]. This theory predicts that both attenuation at the chemical interface and the scattering of electrons on the surface depend on the effective electron path length.

It has been found in [27] that the scattering at the chemical interface is anisotropic, because the coherence loss parameter is anisotropic. It should be pointed out that the optical phenomena in the layered spherical nanoobjects of the different morphology has already been studied in a number of works. Thus, the works [28, 29] deal with the plasmonic phenomena in bimetallic nanoparticles, and the works [30–32] deal with the plasmonic phenomena in the composite particles of the type "metallic core – dielectric shell" and "dielectric core – metallic shell".

However, the problem connected with the excitation of the surface plasmonic resonances in the metallic nanoparticles, covered with adsorbate layer, has not been considered in the literature. In this regard, the study of the frequency dependences for the longitudinal and transverse parameter of the coherence loss under the scattering at the chemical interface, as well as the construction of the plasmonic effects theory in the nanoparticle of the type "metallic core – layer of adsorbed molecules" taking into account the indicated scattering mechanisms is an actual problem.

BASIC RELATIONS

Let us consider the spherical metallic nanoparticle with the radius R_c, covered with the adsorbed molecules layer with the thickness t (the total radius of the composite nanoparticle $R = R_c + t$) which is situated in the dielectric environment with the permittivity ϵ_m (Fig. 1).
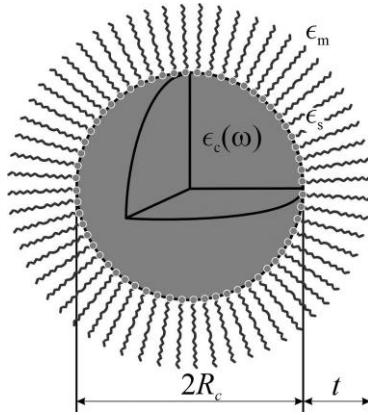

Fig. 1. Geometry of the problem

Let us assume that the following assumptions are valid.

1. From one hand, the metallic core is small, that is why the contribution of the radiation attenuation into the effective relaxation rate can be neglected, and, from an other hand, the sizes of metallic core are such that the quantum size effects in the metallic core do not manifest themselves. This fact gives an opportunity to study the optical properties of the nanoparticle, which is under the consideration, in the frameworks of the classical electrodynamics, and also to assume that three mechanisms additively contribute into the effective relaxation rate: bulk and surface scattering, and the scattering at the interface between the metallic core and adsorbate.

2. Moreover, the scattering at the chemical interface due to the transition of metal electrons to the loosened levels of adsorbate molecules is anisotropic.

Let us consider the relations for the absorption cross-section and scattering cross-section of the composite nanoparticle as the starting point for the study

$$C_@^{abs} = \frac{\omega}{c}\sqrt{\epsilon_m}\left(\frac{2}{3}\operatorname{Im}\alpha_@^\perp + \frac{1}{3}\operatorname{Im}\alpha_@^\parallel\right); \qquad (1)$$

$$C_@^{sca} = \frac{1}{6\pi}\left(\frac{\omega}{c}\right)^4 \epsilon_m^2\left(\frac{2}{3}\left|\alpha_@^\perp\right|^2 + \frac{1}{3}\left|\alpha_@^\parallel\right|^2\right), \qquad (2)$$

where ω is the incident light frequency; c is the velocity of light, and the components of the polarizability tensor for the two-layer nanoparticle

$$\alpha_@^{\perp(\parallel)} = V\frac{\epsilon_@^{\perp(\parallel)} - \epsilon_m}{\epsilon_@^{\perp(\parallel)} + 2\epsilon_m}. \qquad (3)$$

In the expression (3) V is the volume of the nanoparticle, $\epsilon_@^{\perp(\parallel)}$ is the diagonal components of the dielectric tensor of the composite nanoparticle, which are determined by the relation

$$\epsilon_@^{\perp(\parallel)} = \epsilon_s\frac{1 + 2\beta_c\delta_@^{\perp(\parallel)}}{1 - \beta_c\delta_@^{\perp(\parallel)}}, \qquad (4)$$

where

$$\delta_@^{\perp(\parallel)} = \frac{\epsilon_c^{\perp(\parallel)} - \epsilon_s}{\epsilon_c^{\perp(\parallel)} + 2\epsilon_s}, \qquad (5)$$

In formulas (4) and (5): ϵ_s is the dielectric permittivity of the adsorbed layer substance (shell); $\beta_c = (R_c/R)^3$ is the volumetric content of metal, and the transverse (longitudinal) components of the dielectric tensor of the metallic core have the form

$$\epsilon_c^{\perp(\parallel)}(\omega) = \epsilon^\infty - \frac{\omega_p^2}{\omega\left(\omega + i\gamma_{eff}^{\perp(\parallel)}\right)}, \qquad (6)$$

where ϵ^∞ is the contribution of the crystal lattice into the dielectric function; ω_p is the plasmonic frequency, and the expression for the effective relaxation rate has the form

$$\gamma_{eff}^{\perp(\parallel)} = \gamma_{bulk} + \gamma_s + \gamma_{CID}^{\perp(\parallel)}. \qquad (7)$$

The surface relaxation rate can be written down as [33]

$$\gamma_s = \mathscr{A}_{size}\frac{v_F}{R_c}, \qquad (8)$$

where v_F is the Fermi velocity of electrons;

$$\mathscr{A}_{size} = \frac{1}{4}\left(\frac{\omega_p}{\omega}\right)^2\left[1 - \frac{2\nu_s}{\omega}\sin\frac{\omega}{\nu_s} + \frac{2\nu_s^2}{\omega^2}\left(1 - \cos\frac{\omega}{\nu_s}\right)\right] \qquad (9)$$

– an effective parameter, which describes the degree of coherence loss under the scattering of electrons on the surface of the nanoparticle, $\nu_s = \nu_F/2R_c$ – the frequency of the individual oscillations of electron.

The last addend in formula (7) describes the relaxation processes, caused by the presence of the interface "metal – adsorbed layer"

$$\gamma_{CID}^{\perp(\parallel)} = \mathscr{A}_{\perp(\parallel)}^{interface}\frac{\nu_F}{R_c}, \qquad (10)$$

where the frequency dependences for the coefficient $\mathscr{A}_{\perp(\parallel)}^{interface}$ are determined by the formulas [27]

$$\mathscr{A}_{\perp}^{interface} = 4n_a\frac{\omega_{sp}}{\hbar\nu_F}\frac{\epsilon_s}{\epsilon^\infty + 2\epsilon_s}\mathscr{F}_{\perp}(\omega); \qquad (11)$$

$$\mathscr{A}_{\parallel}^{interface} = \frac{3}{8}n_a\sigma_0\left(\frac{1 + 2\epsilon_s}{\epsilon^\infty + 2\epsilon_s}\right)^2\mathscr{F}(\omega). \qquad (12)$$

In formulas (11) and (12): $\sigma_0 = 64\omega_F Q/3\pi n_e\nu_F$ (n_e is the concentration of electrons, Q is the number which depends on the symmetry of the adsorbed resonance state, $Q = 0.2$ for s- and p_z-states, $Q \approx 0.33$ – for p_x- and p_y- states); $\omega_F = \varepsilon_F/\hbar$ (ε_F is the Fermi energy); n_a is the surface density of adsorbed atoms; ω_{sp} – frequency of SPR, and

$$\mathscr{F}(\hbar\omega) = \frac{\pi}{4\varepsilon_F\hbar\omega}\int\limits_{\varepsilon_F-\hbar\omega}^{\varepsilon_F}d\varepsilon\Big[\varepsilon\Gamma_a\varrho_a(\varepsilon + \hbar\omega) +$$

$$+ (\varepsilon + \hbar\omega)\Gamma_a\varrho_a(\varepsilon)\Big];$$

$$(13)$$

$$\mathscr{F}_{\perp}(\hbar\omega) = \frac{(ed)^2}{2\epsilon_0}\int\limits_{\varepsilon_F-\hbar\omega}^{\varepsilon_F}d\varepsilon\varrho_a(\varepsilon)\varrho_a(\varepsilon + \hbar\omega); \qquad (14)$$

where

$$\varrho_a(\varepsilon) = \frac{1}{\pi}\frac{\Gamma_a/2}{(\varepsilon - \varepsilon_a)^2 + (\Gamma_a/2)^2}, \qquad (15)$$

is the localized density of the states, which are induced by adsorbate, ε_a and Γ_a are an amplitude and the width of the spectral lines correspondingly; d is the distance between the center of the adsorbed molecule and the image plane.

After the substitution (15) into (13) we obtain

$$\mathscr{F}(\hbar\omega) = \frac{\Gamma_a^2}{8\varepsilon_F\hbar\omega}\left\{\int\limits_{\varepsilon_F-\hbar\omega}^{\varepsilon_F}\frac{\varepsilon d\varepsilon}{(\varepsilon + \hbar\omega - \varepsilon_a)^2 + (\Gamma_a/2)^2} + \right.$$

$$\left. + \int\limits_{\varepsilon_F-\hbar\omega}^{\varepsilon_F}\frac{(\varepsilon + \hbar\omega)d\varepsilon}{(\varepsilon - \varepsilon_a)^2 + (\Gamma_a/2)^2}\right\} = \frac{\Gamma_a^2}{8\varepsilon_F\hbar\omega}(\mathscr{I}_1 + \mathscr{I}_2)$$

$$(16)$$

After the calculation of the integrals in (16) we obtain (see Appendix, formulas (A.1) and (A.2),

$$\mathscr{F} = \frac{\Gamma_a^2}{8\varepsilon_F\hbar\omega}\left\{\frac{1}{2}\left[\ln\left((\varepsilon_F + \hbar\omega - \varepsilon_a)^2 + \left(\frac{\Gamma_a}{2}\right)^2\right) - \ln\left((\varepsilon_F - \hbar\omega - \varepsilon_a)^2 + \left(\frac{\Gamma_a}{2}\right)^2\right)\right] + \right.$$

$$+ \frac{2(\hbar\omega + E_a)}{\Gamma_a}\left[\operatorname{arctg}\frac{2(\varepsilon_F - \varepsilon_a)}{\Gamma_a} - \operatorname{arctg}\frac{2(\varepsilon_F - \hbar\omega - \varepsilon_a)}{\Gamma_a}\right] +$$

$$\left. + \frac{2(\hbar\omega - E_a)}{\Gamma_a}\left[\operatorname{arctg}\frac{2(\varepsilon_F - \varepsilon_a)}{\Gamma_a} - \operatorname{arctg}\frac{2(\varepsilon_F + \hbar\omega - \varepsilon_a)}{\Gamma_a}\right]\right\}.$$

Using the formulas for the differences of arctangents and logarithms, we finally obtain

$$\mathscr{F} = \frac{\Gamma_a}{2\varepsilon_F}\operatorname{arctg}\frac{2(\varepsilon_F - \varepsilon_a)}{\Gamma_a} + \frac{\Gamma_a^2}{16\varepsilon_F\hbar\omega}\ln\frac{(\varepsilon_F + \hbar\omega - \varepsilon_a)^2 + (\Gamma_a/2)^2}{(\varepsilon_F - \hbar\omega - \varepsilon_a)^2 + (\Gamma_a/2)^2} -$$

$$- \frac{\Gamma_a}{4\varepsilon_F\hbar\omega}\left[(\hbar\omega + \varepsilon_a)\operatorname{arctg}\frac{2(\varepsilon_F - \hbar\omega - \varepsilon_a)}{\Gamma_a} + (\hbar\omega - \varepsilon_a)\operatorname{arctg}\frac{2(\varepsilon_F + \hbar\omega - \varepsilon_a)}{\Gamma_a}\right].$$

$$(17)$$

After the substitution of the result of the integration (17) into the expression (11) we obtain

$$\mathscr{A}_{\parallel}^{\text{interface}} = \frac{3\Gamma_a}{16\varepsilon_F} n_a \sigma_0 \left(\frac{1+2\epsilon_s}{\epsilon^{\infty}+2\epsilon_s}\right)^2 \left\{ \text{arctg}\frac{2(\varepsilon_F - \varepsilon_a)}{\Gamma_a} + \right.$$

$$+ \frac{\Gamma_a}{8\hbar\omega}\ln\frac{(\varepsilon_F + \hbar\omega - \varepsilon_a)^2 + (\Gamma_a/2)^2}{(\varepsilon_F - \hbar\omega - \varepsilon_a)^2 + (\Gamma_a/2)^2} - \frac{1}{2\hbar\omega} \times$$

$$\times \left[(\hbar\omega + \varepsilon_a)\text{arctg}\frac{2(\varepsilon_F - \hbar\omega - \varepsilon_a)}{\Gamma_a} + \right.$$

$$\left.\left. + (\hbar\omega - \varepsilon_a)\text{arctg}\frac{2(\varepsilon_F + \hbar\omega - \varepsilon_a)}{\Gamma_a} \right]\right\}.$$

(18)

Now let us calculate the value $\mathscr{A}_{\perp}^{\text{interface}}$. In order to do this we substitute the expression (15) into (14), then we substitute the result into (10)

$$\mathscr{A}_{\perp}^{\text{interface}} = \frac{2}{\pi}(ed)^2 n_a \frac{\sigma_0 \epsilon_s \omega_{sp}}{\hbar v_F (\epsilon^{\infty} + 2\epsilon_s)} \times$$

$$\times \left\{ \frac{4}{\Gamma_a}\left(\text{arctg}\frac{2(\varepsilon_F - \hbar\omega - \varepsilon_a)}{\Gamma_a} - \text{arctg}\frac{2(\varepsilon_F - \varepsilon_a)}{\Gamma_a}\right) + \right.$$

$$\left. + \frac{1}{\hbar\omega}\ln\frac{\left[(\varepsilon_F - \hbar\omega - \varepsilon_a)^2 + (\Gamma_a/2)^2\right]\left[(\varepsilon_F - \hbar\omega - \varepsilon_a)^2 + (\Gamma_a/2)^2\right]}{\left[(\varepsilon_F - \varepsilon_a)^2 + (\Gamma_a/2)^2\right]^2} \right\}.$$

(20)

Let us find the expression for the frequency of the surface plasmonic resonance using the condition of the equality to zero of the denominator of the expression (3) in non-dissipative approximation ($\gamma_{\text{eff}} = 0$). Using the expressions (4) and (5), we obtain

$$(\epsilon_c + 2\epsilon_s)(\epsilon_s + 2\epsilon_m) + 2\beta_c(\epsilon_c - \epsilon_s)(\epsilon_s - \epsilon_m) = 0. \quad (21)$$

Using the formulas (6) and (21), we obtain

$$\epsilon^{\infty} - \frac{\omega_p^2}{\omega_{sp}^2} = -2\epsilon_s\frac{(1-2\beta_c)\epsilon_s + 2(1+\beta_c)\epsilon_m}{(1+2\beta_c)\epsilon_s + 2(1-\beta_c)\epsilon_m},$$

or finally

$$\omega_{sp} = \frac{\omega_p}{\sqrt{\epsilon^{\infty} + 2\epsilon_s\frac{(1-2\beta_c)\epsilon_s + 2(1+\beta_c)\epsilon_m}{(1+2\beta_c)\epsilon_s + 2(1-\beta_c)\epsilon_m}}}. \quad (22)$$

$$\mathscr{A}_{\perp}^{\text{interface}} = \frac{(ed\Gamma_a)^2}{2\pi^2\epsilon_0} n_a \frac{\epsilon_s}{\epsilon^{\infty}+\epsilon_s} \frac{\sigma_0\omega_{sp}}{\hbar v_F} \times$$

$$\times \int_{\varepsilon_F - \hbar\omega}^{\varepsilon_F} \frac{d\varepsilon}{\left[(\varepsilon - \varepsilon_a)^2 + (\Gamma_a/2)^2\right]\left[(\varepsilon + \hbar\omega - \varepsilon_a)^2 + (\Gamma_a/2)^2\right]} =$$

$$= \frac{(ed\Gamma_a)^2}{2\pi^2\epsilon_0} n_a \frac{\epsilon_s}{\epsilon^{\infty}+\epsilon_s} \frac{\sigma_0\omega_{sp}}{\hbar v_F} \mathscr{I}_3.$$

(19)

After the calculation of the integral $\mathscr{I}_3$ (see Appendix), we obtain the following expression for the parameter $\mathscr{A}_{\perp}^{\text{interface}}$:

Thereafter, the relations (1)–(3) taking into account formulae (4)–(10), (18), (20), (22) are used in order to obtain the numerical results.

THE RESULTS OF THE CALCULATIONS AND THE DISCUSSION

The calculations have been performed for the nanoparticles of the different radius and of different metals, covered with oleylamine layer (OAm) of the different thickness, when the composite structure $\text{Me}@\text{OAm}$ is situated in the different environments. The parameters, used in the calculations, are given in Tables 1–3, the distance between the center of adsorbed molecule and the image plane $d = 10$ nm.

Fig. 2 shows the frequency dependences for the real and imaginary parts and for the module of the longitudinal component of the polarizability tensor for Au nanoparticles of the different radius, covered with oleylamine layer

of the fixed thickness. The curves $\mathrm{Re}\,\alpha_@^{\parallel}(\hbar\omega)$ have closely located maximum and minimum and $\mathrm{Re}\,\alpha_@^{\parallel}(\hbar\omega)$ itself is alternating function of the frequency (Fig. 2 *a*). Differing from $\mathrm{Re}\,\alpha_@^{\parallel}(\hbar\omega)$, the function $\mathrm{Im}\,\alpha_@^{\parallel}(\hbar\omega)$ is the positive defined function and has one extreme (maximum), which corresponds to the surface plasmonic resonance (Fig. 2 *b*). It should be pointed out that the greater the radius is (the content of the metallic fraction in the composite nanoparticle), the more expressed are the extremes of the real and imaginary parts $\alpha_@^{\parallel}$, but their location does not change (that is the

frequency of the surface plasmonic resonance remains constant). The frequency dependences for the module of the longitudinal component of the polarizability tensor have two extremes (Fig. 2 *c*), and, moreover, the maximum coincides with the maximum $\mathrm{Im}\,\alpha_@^{\parallel}(\hbar\omega)$ (is reached under the frequency of SPR), and the minimum is located in the near ultraviolet range. Such location of the minimums $\left|\alpha_@^{\parallel}(\hbar\omega)\right|$ is associated with the fact that $\mathrm{Re}\,\alpha_@^{\parallel}\approx 0$, and $\mathrm{Im}\,\alpha_@^{\parallel}$ rapidly decreases in the indicated spectral range.

Table 1. Parameters of metals (for example, [31, 34] and the references therein)

Parameters	Metals				
	Au	**Ag**	**Cu**	**Pd**	**Pt**
n_e, 10^{22} sm^{-3}	5.91	5.85	17.2	2.53	9.1
ϵ^{∞}	9.84	3.70	12.03	2.52	4.42
$\hbar\omega_p$, eV	9.07	9.17	12.6	9.7	15.2
$\hbar\gamma_{\mathrm{bulk}}$, eV	0.023	0.016	0.024	0.091	0.069
ε_{F}, eV	5.59	5.72	7.56	8.49	13.6
v_{F}, 10^6 m/s	1.41	1.49	1.34	2.84	2.98

Table 2. Parameters of dielectrics [35, 36]

Substance	Air	Toluene	TiO$_2$	C$_{60}$
ϵ_{m}	1	2.24	4.0	6.0

Table 3. Parameters of adsorbate [36]

n_a, sm^{-2}	$\varepsilon_{\mathrm{F}}-\varepsilon_a$, eV	Γ_a, eV	T_s
$1.27\cdot 10^{12}$	1	1	2.13

Fig. 3 shows the frequency dependences for the real and imaginary parts and for the module of the transverse component of the polarizability tensor. Let us point out that the behavior of these dependences significantly differs from the behavior of the curves $\mathrm{Re}\,\alpha_@^{\parallel}(\hbar\omega)$, $\mathrm{Im}\,\alpha_@^{\parallel}(\hbar\omega)$ and $\left|\alpha_@^{\parallel}(\hbar\omega)\right|$. Namely, all these dependencies have the weakly expressed maximum in the far infrared range of the spectrum, but as for the rest part of the spectrum $\mathrm{Re}\,\alpha_@^{\perp}(\hbar\omega)$, $\mathrm{Im}\,\alpha_@^{\perp}(\hbar\omega)$ and $\left|\alpha_@^{\perp}(\hbar\omega)\right|$ are practically independent on the frequency.

The Fig. 4 shows the curves of the frequency dependences for the absorption cross-section and the scattering cross-section. It should be pointed out that if the dependences $C_@^{\mathrm{sca}}(\hbar\omega)$ have one maximum then the number of the maximas $C_@^{\mathrm{abs}}(\hbar\omega)$ depends on the size of the particle. It can be explained by the fact that $C_@^{\mathrm{abs}}\sim\left(2\,\mathrm{Im}\,\alpha_@^{\perp}+\mathrm{Im}\,\alpha_@^{\parallel}\right)$. Hence, the absorption cross-section can reach the maxima when $\mathrm{Im}\,\alpha_@^{\parallel}(\hbar\omega)$ or $\mathrm{Im}\,\alpha_@^{\perp}(\hbar\omega)$ reach the maxima (Fig. 2 *b* and 3 *b*). The maxima $\max\left[\mathrm{Im}\,\alpha_@^{\perp}(\hbar\omega)\right]$ appears under the increase of

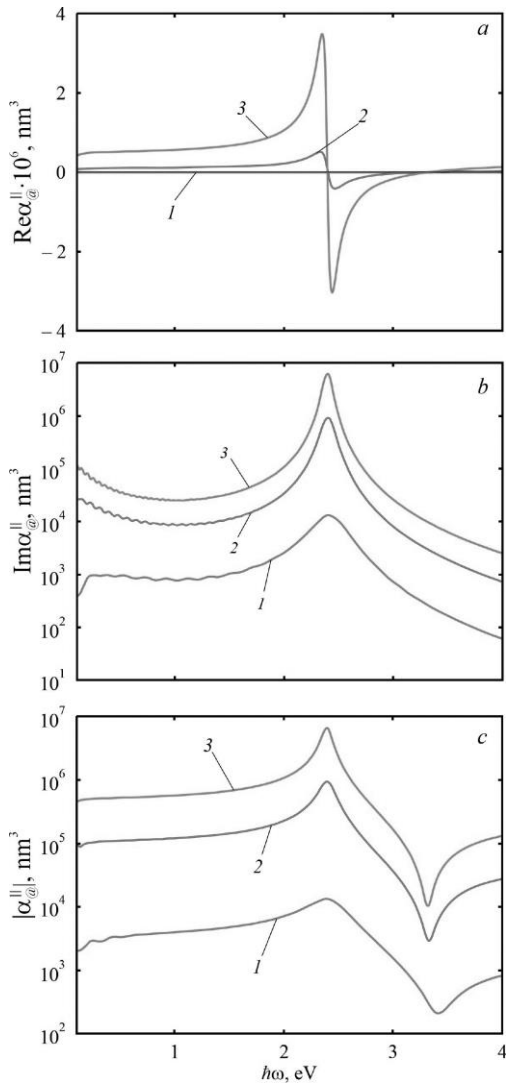the metallic core, hence, the second maxima $C_@^{abs}$ also appears in this case.

Fig. 2. The frequency dependences for the real (*a*) and imaginary (*b*) parts, and for the module (*c*) of the longitudinal component of the polarizability tensor for the nanoparticles Au@OAm of the different radius in toluene: *1* – $R_c = 10$ nm; *2* – $R_c = 30$ nm; *3* – $R_c = 50$ nm at the $t = 5$ nm

Fig. 5 shows the results of calculations for the absorption cross-section and the scattering cross-sections for the nanoparticles of the same size with the cores of different metals. The curves $C_@^{abs}(\hbar\omega)$ and $C_@^{sca}(\hbar\omega)$ have the same particularities as the similar curves in Fig 4. It should be pointed out that if the maximums of the absorption cross-section and the scattering cross-section in the optical and ultraviolet parts

of the spectrum for the particles with the cores of different metals are reached under the frequencies which significantly differ from each other, then the frequencies, which correspond to the maxima in the infrared range, differ insignificantly.
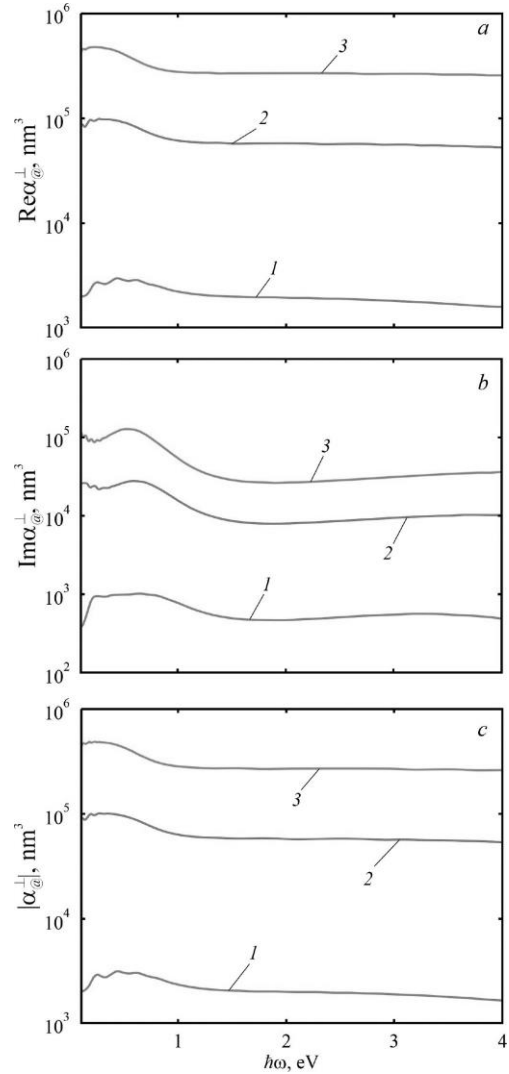

Fig. 3. The frequency dependences for the real (*a*) and imaginary (*b*) parts, and for the module (*c*) of the transverse component of the polarizability tensor for the nanoparticles Au@OAm at the same values of the parameters, as in Fig. 2

It can be explained by the fact that the difference in location of the strongly expressed maxima is associated with the differences between the frequencies of bulk plasmons and the contribution of the crystal lattice into the dielectric permittivity for different metals, while the weakly expressed maximum is associated

with the capability of adsorbate to induce the local density of the states. The results of the calculations of the frequency dependences for the absorption cross-section for the particle of the fixed size with golden core under the different values $\Delta\varepsilon = \varepsilon_F - \varepsilon_a$ confirm such explanation (Fig. 6 *a*). Thus, with the increase $\Delta\varepsilon$ in the sequence of the curves $1\rightarrow2\rightarrow3\rightarrow4$ one observes "blue" shift of $\max\left[C_@^{abs}\right]$ into the near infrared range, however, the maximum itself becomes less expressed, whereas neither location of the maximum nor its amplitude in the optical range does not change.
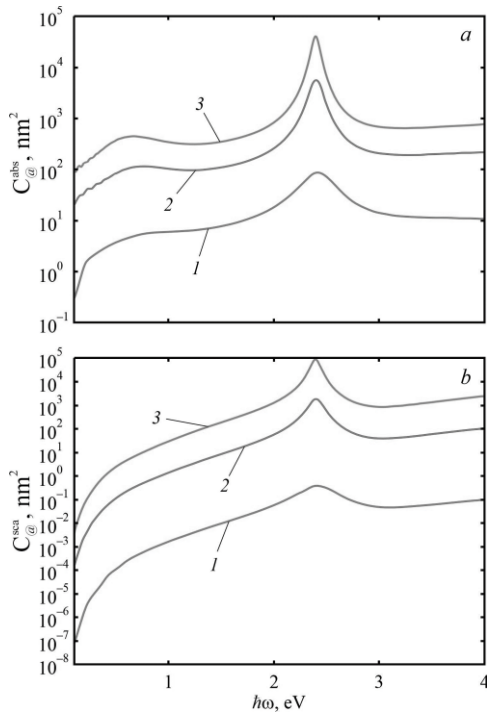

Fig. 4. The frequency dependences for the absorption cross-section (*a*) and scattering cross-section (*b*) for the nanoparticles Au@OAm at the same values of the parameters, as in Fig. 2

Fig. 6 shows the curves of the frequency dependences for the absorption cross-section for the particles of the fixed size with golden core, which are situated in dielectrics with the different permittivity. The results of the calculation demonstrate "red" shift of the maximums of the absorption cross-section with small increase in their amplitude under the increase in T_m.
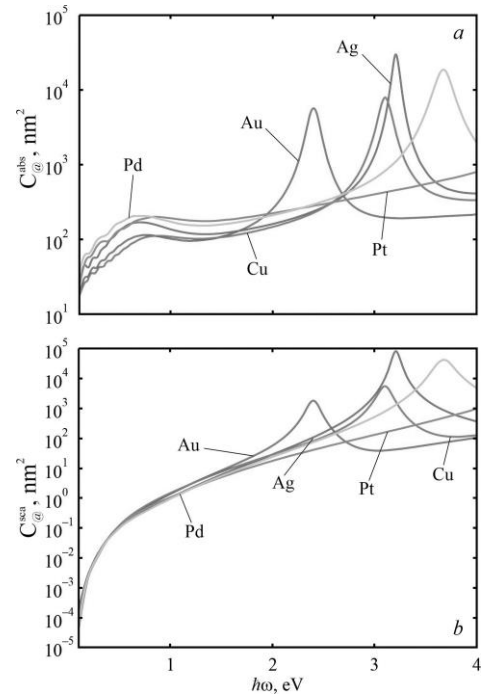

Fig. 5. The frequency dependences for the absorption cross-section (*a*) and scattering cross-section (*b*) for the nanoparticles Me@OAm ($R_c = 30$ nm; $t = 5$ nm) in toluene
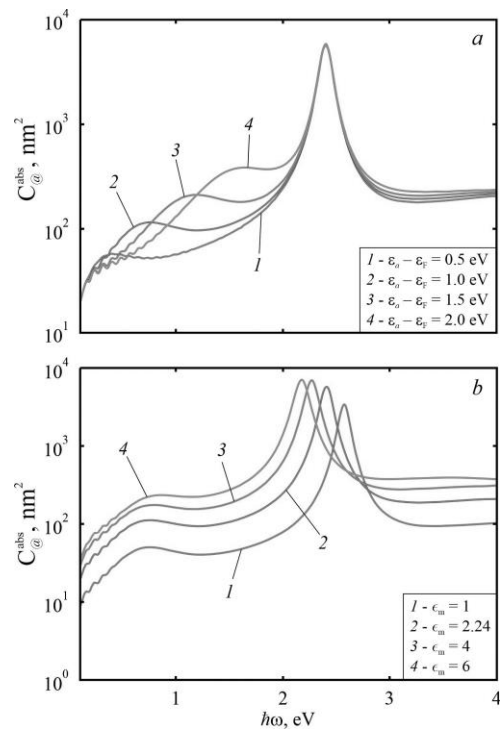

Fig. 6. The frequency dependences for the absorption cross-sections of the nanoparticles Au@OAm ($R_c = 30$ nm; $t = 5$ nm) under the different values $\Delta\varepsilon = \varepsilon_F - \varepsilon_a$ in toluene (*a*) and in the different dielectric media at the $\Delta\varepsilon = 1$ eV (*b*)

In conclusion, in should be noted that the low-amplitude oscillations on the curves 2 *b*, *c*, 3, 4 *a*, 5 *a* and 6 in red and infrared ranges of the spectrum are caused by the kinetic effects, which give the oscillating contribution into the surface relaxation rate.

CONCLUSIONS

The classical theory of the optical absorption by the spherical nanoparticles of metal taking into account the influence of the layer of molecules, adsorbed on its surface, on the relaxation processes has been modified.

It has been shown that the increase in content of metallic fraction in the composite nanoparticle results in the increase in the extreme values of the real and imaginary parts and module of the longitudinal component of the polarizability tensor, and also in the increase in the maximum value of the absorption cross-section and scattering cross-section, that is in the increase in the absorption and scattering at the frequency of the surface plasmonic resonance.

It has been demonstrated that the curves of the frequency dependences for the real and imaginary parts and module of the transverse component of the polarizability tensor qualitatively differ from the similar curves for the longitudinal component of the polarizability tensor by the presence of the weakly expressed maximum in the far infrared region of the spectrum, the appearance of which is associated with the local density of the states, induced by adsorbate.

It has been found the existence of the small oscillations of the absorption cross-section of the real and imaginary parts and the module of the longitudinal and transverse components of the polarizability tensor, caused by the contribution of the surface relaxation.

It has been shown that the location of the maxima of the absorption cross-section and scattering cross-section in the visible and ultraviolet ranges of the spectrum for the composite nanoparticles of the fixed sizes with the cores of different metals significantly differs due to the difference in such parameters of metals as the frequency of bulk plasmons and the contribution of ion core into the dielectric permittivity.

It has been demonstrated that the location and the amplitude of the maxima of the absorption cross-section for the nanoparticle of the fixed size and the content depend on the properties of the medium, in which the nanoparticle is situated. Thus, the increase in the permittivity of dielectric results in the increase in the amplitude of the maxima, and the maxima itself shifts into the domain of the smaller frequencies.

APPENDIX. THE CALCULATION OF THE INTEGRALS

Calculating the integrals $\mathscr{I}_1$ and $\mathscr{I}_2$ in (16), we obtain

$$\mathscr{I}_1 = \int\limits_{\varepsilon_F - \hbar\omega}^{\varepsilon_F} \frac{E\,dE}{\left(E + \hbar\omega - E_a\right)^2 + \left(\Gamma_a/2\right)^2} = \int\limits_{\varepsilon_F - \hbar\omega}^{\varepsilon_F} \frac{\left(E + \hbar\omega - E_a\right)d\left(E + \hbar\omega - E_a\right)}{\left(E + \hbar\omega - E_a\right)^2} -$$

$$- \left(\hbar\omega - E_a\right) \int\limits_{\varepsilon_F - \hbar\omega}^{\varepsilon_F} \frac{d\left(E + \hbar\omega - E_a\right)}{\left(E + \hbar\omega - E_a\right)^2 + \left(\Gamma_a/2\right)^2} =$$

$$= -\frac{2\left(\hbar\omega - E_a\right)}{\Gamma_a} \left\{ \operatorname{arctg} \frac{2\left(\varepsilon_F + \hbar\omega - E_a\right)}{\Gamma_a} - \operatorname{arctg} \frac{2\left(\varepsilon_F - E_a\right)}{\Gamma_a} \right\} +$$

$$+ \frac{1}{2} \left\{ \ln\left(\left(\varepsilon_F + \hbar\omega - E_a\right)^2 + \left(\frac{\Gamma_a}{2}\right)^2 \right) - \ln\left(\left(\varepsilon_F - E_a\right)^2 + \left(\frac{\Gamma_a}{2}\right)^2 \right) \right\};$$

(A.1)

$$\mathscr{I}_2 = \int\limits_{\varepsilon_F - \hbar\omega}^{\varepsilon_F} \frac{(E + \hbar\omega) dE}{(E - E_a)^2 + (\Gamma_a/2)^2} = \int\limits_{\varepsilon_F - \hbar\omega}^{\varepsilon_F} \frac{(E - E_a) d(E - E_a)}{(E - E_a)^2 + (\Gamma_a/2)^2} +$$

$$+ (\hbar\omega + E_a) \int\limits_{\varepsilon_F - \hbar\omega}^{\varepsilon_F} \frac{d(E - E_a)}{(E - E_a)^2 + (\Gamma_a/2)^2} =$$

$$= \frac{2(\hbar\omega + E_a)}{\Gamma_a} \left\{ \operatorname{arctg} \frac{2(\varepsilon_F - E_a)}{\Gamma_a} - \right.$$

$$\left. - \operatorname{arctg} \frac{2(\varepsilon_F - \hbar\omega - E_a)}{\Gamma_a} \right\} + \frac{1}{2} \left\{ \ln\left((\varepsilon_F - E_a)^2 + \left(\frac{\Gamma_a}{2}\right)^2 \right) - \right.$$

$$\left. - \ln\left((\varepsilon_F - \hbar\omega - E_a)^2 + \left(\frac{\Gamma_a}{2}\right)^2 \right) \right\}. \tag{A.2}$$

Now the integral $\mathscr{I}_3$ in the expression (18). In order to do this let us move to a new variable $\tilde{\varepsilon} = \varepsilon - \varepsilon_a$. As the result, the integral has the form

$$\mathscr{I}_3 = \int\limits_{\varepsilon_F - \hbar\omega - \varepsilon_a}^{\varepsilon_F - \varepsilon} \frac{d\tilde{\varepsilon}}{\left[\tilde{\varepsilon}^2 + (\Gamma_a/2)^3 \right]\left[(\tilde{\varepsilon} + \hbar\omega)^2 + (\Gamma_a/2)^2 \right]}. \tag{A.3}$$

Let us use the method of undetermined coefficients for the calculation of the integrals in (A.3)

$$\int\limits_{\varepsilon_F - \hbar\omega - \varepsilon_a}^{\varepsilon_F - \varepsilon_a} \frac{d\tilde{\varepsilon}}{\left[\tilde{\varepsilon}^2 + (\Gamma_a/2)^2 \right]\left[(\tilde{\varepsilon} + \hbar\omega)^2 + (\Gamma_a/2)^2 \right]} =$$

$$\int\limits_{\varepsilon_F - \hbar\omega - \varepsilon_a}^{\varepsilon_F - \varepsilon_a} \frac{A\tilde{\varepsilon} + B}{\tilde{\varepsilon}^2 + (\Gamma_a/2)^2} d\tilde{E} + \int\limits_{\varepsilon_F - \hbar\omega - \varepsilon_a}^{\varepsilon_F - \varepsilon_a} \frac{C\tilde{\varepsilon} + D}{(\tilde{\varepsilon} + \hbar\omega)^2 + (\Gamma_a/2)^2} d\tilde{\varepsilon} = \mathscr{I}_3^{(1)} + \mathscr{I}_3^{(2)}. \tag{A.4}$$

In order to determine these coefficients, let us equate the expressions at the different degrees $\tilde{\varepsilon}$ in the left-hand side and the right-hand side of the expression (A.4)

$$(A\tilde{\varepsilon} + B)\left[(\tilde{\varepsilon} + \hbar\omega)^2 + \left(\frac{\Gamma_a}{2}\right)^2 \right] + (C\tilde{\varepsilon} + D)\left[\tilde{\varepsilon}^2 + \left(\frac{\Gamma_a}{2}\right)^2 \right] = 1. \tag{A.5}$$

Thus, we obtain the system of equations from (A.5).

$$\begin{cases} A + C = 0; \\ 2\hbar\omega A + B + D = 0; \\ \left(\frac{\Gamma_a^2}{4} + \hbar^2\omega^2\right) A + 2\hbar\omega B + \frac{\Gamma_a^2}{4} C = 0; \\ \left(\frac{\Gamma_a^2}{4} + \hbar^2\omega^2\right) B + \frac{\Gamma_a^2}{4} D = 1. \end{cases} \tag{A.6}$$

Solving the system (A.6), we obtain

$$A = -\frac{2}{\hbar\omega\left(\hbar^2\omega^2 + \Gamma_a^2\right)}; \quad B = \frac{1}{\hbar^2\omega^2 + \Gamma_a^2}; \quad C = \frac{2}{\hbar\omega\left(\hbar^2\omega^2 + \Gamma_a^2\right)}; \quad D = \frac{3}{\hbar^2\omega^2 + \Gamma_a^2}. \tag{A.7}$$

Let us calculate the integrals $\mathscr{I}_3^{(1)}$ and $\mathscr{I}_3^{(2)}$:

$$\mathscr{I}_3^{(1)} = -\frac{2}{\hbar\omega\Gamma_a^2}\int\limits_{\varepsilon_F-\hbar\omega-\varepsilon_a}^{\varepsilon_F-\varepsilon_a}\frac{\tilde{\varepsilon}\,d\tilde{\varepsilon}}{\tilde{\varepsilon}^2+(\Gamma_a/2)^2} = -\frac{1}{\hbar\omega\Gamma_a^2}\ln\frac{(\varepsilon_F-\varepsilon_a)^2+(\Gamma_a/2)^2}{(\varepsilon_F-\hbar\omega-\varepsilon_a)^2+(\Gamma_a/2)^2};$$

$$\mathscr{I}_3^{(2)} = \int\limits_{\varepsilon_F-\hbar\omega-\varepsilon_a}^{\varepsilon_F-\varepsilon_a}\frac{\left(\dfrac{2}{\hbar\omega\Gamma_a^2}\tilde{\varepsilon}+\dfrac{4}{\Gamma_a^2}\right)d\tilde{\varepsilon}}{(\tilde{\varepsilon}+\hbar\omega)^2+(\Gamma_a/2)^2} = \frac{4}{\Gamma_a^2}\int\limits_{\varepsilon_F-\hbar\omega-\varepsilon_a}^{\varepsilon_F-\varepsilon_a}\frac{d(\tilde{\varepsilon}+\hbar\omega)}{(\tilde{\varepsilon}+\hbar\omega)^2+(\Gamma_a/2)^2}+$$

$$+\frac{2}{\hbar\omega\Gamma_a^2}\int\limits_{\varepsilon_F-\hbar\omega-\varepsilon_a}^{\varepsilon_F-\varepsilon_a}\frac{(\tilde{\varepsilon}+\hbar\omega)d(\tilde{\varepsilon}+\hbar\omega)}{(\tilde{\varepsilon}+\hbar\omega)^2+(\Gamma_a/2)^2} - \frac{2}{\Gamma_a^2}\int\limits_{\varepsilon_F-\hbar\omega-\varepsilon_a}^{\varepsilon_F-\varepsilon_a}\frac{d(\tilde{\varepsilon}+\hbar\omega)}{(\tilde{\varepsilon}+\hbar\omega)^2+(\Gamma_a/2)^2} =$$

$$= \frac{4}{\Gamma_a^3}\left(\text{arctg}\frac{(\varepsilon_F+\hbar\omega-\varepsilon_a)}{\Gamma_a}-\text{arctg}\frac{(\varepsilon_F-\varepsilon_a)}{\Gamma_a}\right)+\frac{1}{\hbar\omega\Gamma_a^2}\ln\frac{(\varepsilon_F+\hbar\omega-\varepsilon_a)^2+(\Gamma_a/2)^2}{(\varepsilon_F-\varepsilon_a)^2+(\Gamma_a/2)^2}.$$

Hence, the integral $\mathscr{I}_3$ is equal to

$$\mathscr{I}_3 = \frac{4}{\Gamma_a^3}\left(\text{arctg}\frac{2(\varepsilon_F+\hbar\omega-\varepsilon_a)}{\Gamma_a}-\text{arctg}\frac{2(\varepsilon_F-\varepsilon_a)}{\Gamma_a}\right)+\frac{1}{\hbar\omega\Gamma_a^2}\times$$
$$\times\ln\frac{\left[(\varepsilon_F+\hbar\omega-\varepsilon_a)^2+(\Gamma_a/2)^2\right]\left[(\varepsilon_F-\hbar\omega-\varepsilon_a)^2+(\Gamma_a/2)^2\right]}{\left[(\varepsilon_F-\varepsilon_a)^2+(\Gamma_a/2)^2\right]^2}.$$

(A.8)

Substituting (A.8) into (19), we obtain the formula (20).

Вплив шару адсорбованих молекул на локалізовані поверхневі плазмони в сферичних металевих наночастинках

Н.А. Смирнова, А.В. Коротун, І.М. Тітов

Національний університет «Запорізька політехніка»
вул. Жуковського, 64, Запоріжжя, 69063, Україна, andko@zp.edu.ua
Інститут металофізики ім. Г.В. Курдюмова Національної академії наук України
бульвар Академіка Вернадського, 36, Київ, 03142, Україна
UAD Systems
вул. Олександрівська, 84, Запоріжжя, 69002, Україна

В роботі досліджено вплив шару адсорбованих молекул на оптичні характеристики сферичних металевих наночастинок. З цією метою у виразах для швидкості релаксації наявний додатковий член, що враховує розсіювання електронів на межі металу з адсорбатом. Отримано аналітичні вирази для частотних залежностей параметра втрати когерентності за рахунок розсіювання на межі поділу «метал – адсорбований шар». Встановлено, що наявність адсорбованих молекул призводить до анізотропії розсіювання електронів, і, як наслідок, анізотропії оптичного відгуку подібних систем. Результатом зазначеної анізотропії є поява у частотних залежностях оптичних характеристик додаткового максимуму в інфрачервоній області спектра. Проаналізовано еволюцію частотних залежностей компонент тензора поляризованості і перерізів поглинання та розсіювання двошарових сферичних наночастинок типу «метал – адсорбат» при зміні їхніх геометричних параметрів. Показано, що слабко виражений максимум дійсної, уявної частин і модуля поперечної компоненти тензора поляризованості, а також перерізів поглинання та розсіювання в інфрачервоній області спектра виникає внаслідок індукування адсорбатом локальної густини станів. Встановлено причину зсуву максимумів перерізів поглинання та розсіювання для наночастинок постійних розмірів із ядрами різних металів. Продемонстровано існування дрібномасштабних осциляцій на

частотних залежностях компонент тензора поляризованості і перерізів поглинання та розсіювання, обумовлених осцилюючим внеском поверхневого розсіювання електронів. Доведено залежність положення та величини максимуму перерізу поглинання частинки «метал – адсорбат» із незмінними геометричними параметрами та складом від діелектричної проникності середовища, в якому знаходиться наночастинка.

Ключові слова: *композитна наночастинка, адсорбат, поляризованість, перерізи поглинання і розсіювання, поверхневий плазмонний резонанс, локальна густина станів*

REFERENCES

1. Valsecchi C., Brolo A.G. Periodic metallic nanostructures as plasmonic chemical sensors. *Langmuir.* 2013. **29**(19): 5638.
2. Schatz G.C., Van Duyne R.P. Electromagnetic mechanism of surface-enhanced spectroscopy. In: *Handbook of Vibrational Spectroscopy.* (John Wiley & Sons, Ltd., 2006).
3. Moskovits M. Surface-enhanced Raman spectroscopy: a brief retrospective. *J. Raman Spectrosc.* 2005. **36**(6–7): 485.
4. Barnes W.L., Dereux A., Ebbesen T.W. Surface plasmon subwavelength optics. *Nature.* 2003. **424**(6950): 824830.
5. Noginov M.A., Zhu G., Belgrave A.M., Bakker R., Shalaev V.M., Narimanov E.E., Stout S., Herz E., Suteewong T., Wiesner U. Demonstration of a spaser-based nanolaser. *Nature.* 2009. **460**(7259): 1110.
6. Knight M.W., Sobhani H., Nordlander P., Halas N.J. Photodetection with active optical antennas. *Science.* 2011. **332**(6030): 702.
7. Kakavelakis G., Vangelidis I., Heuer-Jungemann A., Kanaras A.G., Lidorikis E., Stratakis E., Kymakis E. Plasmonic Backscattering Effect in High-Efficient Organic Photovoltaic Devices. *Adv. Energy Mater.* 2016. **6**(2): 1501640.
8. Foerster B., Joplin A., Kaefer K., Celiksoy S., Link S., Sönnichsen C. Chemical Interface Damping Depends on Electrons Reaching the Surface. *ACS Nano.* 2017. **11**(3): 2886.
9. Collins S.S., Wei X., McKenzie T.G., Funston A.M., Mulvaney P. Single Gold Nanorod Charge Modulation in an Ion Gel Device. *Nano Lett.* 2016. **16**(11): 6863.
10. Byers C.P., Hoener B.S., Chang W.S., Link S., Landes C.F. Single-Particle Plasmon Voltammetry (Sppv) for Detecting Anion Adsorption. *Nano Lett.* 2016. **16**(4): 2314.
11. Christopher P., Xin H., Linic S. Visible-Light-Enhanced Catalytic Oxidation Reactions on Plasmonic Silver Nanostructures. *Nat. Chem.* 2011. **3**: 467.
12. Mubeen S., Lee J., Singh N., Krämer S., Stucky G.D., Moskovits M. An Autonomous Photosynthetic Device in which All Charge Carriers Derive from Surface Plasmons. *Nat. Nanotechnol.* 2013. **8**: 247.
13. Naik G.V., Dionne J.A. Photon Upconversion with Hot Carriers in Plasmonic Systems. *Appl. Phys. Lett.* 2015. **107**(13): 133902.
14. Mitsudome T., Kaneda K. Gold Nanoparticle Catalysts for Selective Hydrogenations. *Green Chem.* 2013. **15**(10): 2636.
15. Brongersma M.L., Halas N.J., Nordlander P. Plasmon-Induced Hot Carrier Science and Technology. *Nat. Nanotechnol.* 2015. **10**: 25.
16. Wu K., Chen J., Mcbride J.R., Lian T. Efficient Hot-Electron transfer by a Plasmon-Induced Interfacial Charge-Transfer Transition. *Science.* 2015. **349**(6248): 632.
17. Hartland G.V. Optical Studies of Dynamics in Noble Metal Nanostructures. *Chem. Rev.* 2011. **111**(6): 3858.
18. Hoggard A., Wang L.-Y., Ma L., Fang Y., You G., Olson J., Liu Z., Chang W.-S., Ajayan P.M., Link S. Using the Plasmon Linewidth To Calculate the Time and Efficiency of Electron Transfer between Gold Nanorods and Graphene. *ACS Nano.* 2013. **7**(12): 11209.
19. Olson J., Dominguez-Medina S., Hoggard A., Wang L.-Y., Chang W.-S., Link S. Optical Characterization of Single Plasmonic Nanoparticles. *Chem. Soc. Rev.* 2015. **44**(1): 40.
20. Munechika K., Smith J.M., Chen Y., Ginger D.S. Plasmon Line Widths of Single Silver Nanoprisms as a Function of Particle Size and Plasmon Peak Position. *J. Phys. Chem. C.* 2007. **111**(51): 18906.
21. Kreibig U., Michael V. *Optical Properties of Metal Clusters.* (Berlin: Springer, 1995).
22. Charle K.-P., Frank F., Schulze W. The Optical Properties of Silver Microcrystallites in Dependence on Size and the Influence of the Matrix Environment. *Berichte der Bunsengesellschaft für physikalische Chemie.* 1984. **88**(4): 350.

_____

23. Lohse S.E., Murphy C.J. The Quest for Shape Control: A History of Gold Nanorod Synthesis. *Chem. Mater.* 2013. **25**(8): 1250.
24. Klar T., Perner M., Grosse S., Von Plessen G., Spirkl W., Feldmann J. Surface-Plasmon Resonances in Single Metallic Nanoparticles. *Phys. Rev. Lett.* 1998. **80**(19): 4249.
25. Hövel H., Fritz S., Hilger A., Kreibig U., Vollmer M. Width of Cluster Plasmon Resonances: Bulk Dielectric Functions and Chemical Interface Damping. *Phys. Rev. B*. 1993. **48**(24): 18178.
26. Kusar P., Gruber C., Hohenau A., Krenn J.R. Measurement and Reduction of Damping in Plasmonic Nanowires. *Nano Lett*. 2012. **12**(2): 661.
27. Persson J. Polarizability of Small Spherical Metal Particles: Influence of the Matrix Environment. *Surf. Sci*. 1993. **281**(1−2): 153.
28. Korotun A.V., Koval' A.A., Reva V.I., Titov I.N. Optical Absorption of a Composite Based on Bimetallic Nanoparticles. Classical Approach. *Phys. Met. Metall.* 2019. **120**(11): 1040.
29. Korotun A.V., Koval A.O., Pogosov V.V. Optical parameters of bimetallic nanospheres. *Ukr. J. Phys.* 2021. **66**(6): 518.
30. Korotun A.V., Koval' A.A., Reva V.I. Absorption of Electromagnetic Radiation by Oxide-Coated Spherical Metal Nanoparticles. *J. Appl. Spectrosc.* 2019. **86**(4): 606.
31. Korotun A.V., Koval' A.A. Optical Properties of Spherical Metal Nanoparticles Coated with an Oxide Layer. *Opt. Spectrosc.* 2019. **127**(6): 1161.
32. Korotun A.V., Koval' A.A., Titov I.N. Optical Absorption of a Composite Based on Bilayer Metal–Dielectric Spherical Nanoparticles. *J. Appl. Spectrosc.* 2020. **87**(2): 240.
33. Grigorchuk N.I., Tomchuk P.M. Optical and transport properties of spheroidal metal nanoparticles with account for the surface effect. *Phys. Rev. B*. 2011. **84**(8): 085448.
34. Korotun A.V., Pavlyshche N.I. Cross Sections for Absorption and Scattering of Electromagnetic Radiation by Ensembles of Metal Nanoparticles of Different Shapes. *Phys. Met. Metall.* 2021. **122**(10): 941.
35. Pinchuk A., von Plessen G., Kreibig U. Influence of interband electronic transitions on the optical absorption in metallic nanoparticles. *J. Phys. D: Appl. Phys.* 2004. **37**(22): 3133.
36. Peng S., McMahon J.M., Schatz G.C., Gray S.K., Sun Y. Reversing the size-dependence of surface plasmon resonances. *Proc. Natl. Acad. Sci. USA*. 2010. **107**(33): 14530.